NJC

Accepted Manuscript

This is an *Accepted Manuscript*, which has been through the Royal Society of Chemistry peer review process and has been accepted for publication.

Accepted Manuscripts are published online shortly after acceptance, before technical editing, formatting and proof reading. Using this free service, authors can make their results available to the community, in citable form, before we publish the edited article. We will replace this *Accepted Manuscript* with the edited and formatted *Advance Article* as soon as it is available.

You can find more information about *Accepted Manuscripts* in the Information for Authors.

Please note that technical editing may introduce minor changes to the text and/or graphics, which may alter content. The journal's standard Terms & Conditions and the Ethical guidelines still apply. In no event shall the Royal Society of Chemistry be held responsible for any errors or omissions in this *Accepted Manuscript* or any consequences arising from the use of any information it contains.

ROYAL SOCIETY OF CHEMISTRY

www.rsc.org/njc

NJC

RSCPublishing

ARTICLE

Charge Transfer Aided Selective Sensing and Capture of Picric Acid by Triphenylbenzenes

Cite this: DOI: 10.1039/x0xx00000x

Pratap Vishnoi, Saumik Sen, G. Naresh Patwari*, and Ramaswamy Murugavel*

Received 00th January 2012,
Accepted 00th January 2012

DOI: 10.1039/x0xx00000x

www.rsc.org/

A fluorescent chemo-sensor, 1,3,5-tris(4'-(*N*,*N*-dimethylamino)phenyl)benzene was synthesized by substituting N-H protons of 1,3,5-tris(4'-aminophenyl)benzene with methyl groups. The chemo-sensor shows highly selective and remarkable fluorescence quenching in the presence of picric acid with detection limit of 1.5 ppm. The origin of the selectivity was investigated through absorption, fluorescence emission and ^{1}H NMR spectroscopic techniques. Solid state structure of 1,3,5-tris(4'-(*N*,*N*-dimethylamino)phenyl)benzene and its picric acid complex reveals multiple hydrogen bonds (N-H···O and C-H···O), π-π interaction and electrostatic interactions between 1,3,5-tris(4'-(*N*,*N*-dimethylamino)phenyl)benzene and picric acid. Proton transfer process from picric acid to 1,3,5-tris(4'-(*N*,*N*-dimethylamino)phenyl)benzene results in the formation of picrate anions and triply protonated 1,3,5-tris(4'-(*N*,*N*-dimethylamino)phenyl)benzene species containing dimethylammonium (–$NHMe_2^+$) groups.

1. Introduction

Materials design using non-covalent interactions, such as hydrogen bonding and π-stacking, as crucial cogs is being continuously explored in the field of supramolecular chemistry.[1-3] The complementary nature of the interacting molecules to form such non-covalent interactions can be tuned to achieve selectivity by appropriately modulating the electronic structure. Depending on the nature of the interaction and the constituent involved, this complementarity and the selectivity can then be used in a wide variety of chemo-sensing process.[4]

Due to the simplicity, high selectivity and sensitivity, fluorescent chemo-sensors have found potential applications in the detection of environmentally important analytes such as polynitroaromatic (PNAC) explosives.[4] Fluorescence quenching by photoinduced electron transfer (PET) is the mechanism of sensing which depends on energy gap between LUMOs of the fluorophore and the quencher, and binding efficiency of the fluorophore and the quencher molecules.[5] PNAC analytes are electron-deficient and chemically inert, and prefer to form aromatic π-interactions with the electron-rich aromatic host. The presence of nitro groups can further enhance the complexation through hydrogen bonds with suitable donor groups on the host molecules.

The hydrogen bonding involving functional groups such as hydroxyl, carboxyl and nitro have been extensively investigated and fall into pattern formalized by Etter's rules, provide the framework for complementary and selective binding.[6] Supramolecular fluorophores based on hydroxyl and carboxyl functionalized pyrenes and anthracenes, have been reported to show selective sensing efficiency.[7] Our recent studies have revealed selective sensing of PNAC analytes by 1,3,5-tris(4'-aminophenyl)benzene (TAPB).[8] The concomitant formation of hydrogen bonding between -NH_2 groups of TAPB and -NO_2 groups of PNAC influences the efficiency of the fluorescence quenching process, thereby increasing the sensitivity of detection. To investigate the role of hydrogen bonding of -NH_2 group of TAPB in the sensing mechanism, the supramolecular TAPB fluorophore has been modified to a discrete fluorophore by replacing N-H protons with methyl groups (Chart 1).

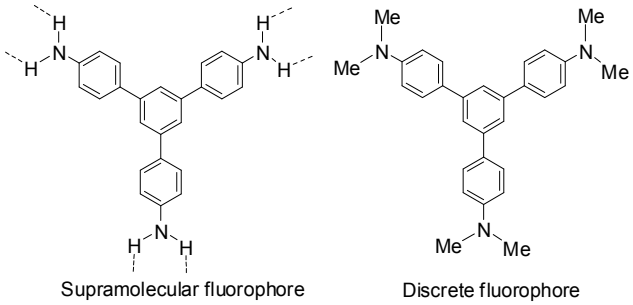

Chart 1. Supramolecular and discrete forms of 1,3,5-triaminophenylbenzene.

Though the discrete fluorophore, 1,3,5-tris(4'-(*N*,*N*-dimethylamino)phenyl)benzene ([(*N*,*N*)Me_2]$_3$TAPB) does not have H-bond donor characteristics, it posses lone pair electrons on the -NMe_2 which can accept protons from polynitroaromatic compounds containing protic groups such as -OH group in picric acid (PA). Considering these factors, in the present investigation, we have demonstrated [(*N*,*N*)Me_2]$_3$TAPB as a chemo-sensor for PA at ppm level detection limit based on fluorescene quenching mechanism. Although PA is a powerful explosive as TNT, only few reports on sensing of PA are available in the literature as compared to that of TNT. PA is also a non-biodegradable environmental pollutant which causes several problems to human health, such as skin irritation, skin allergy, cancer and respiratory system and liver damages.[9] Large quantities of PA are used in pharmaceuticals, dye and fireworks industries as a chemical reagent and released in the environment which eventually enters in the food chain.[10] Thus

the development of fast and selective method for the detection of PA is highly desirable.[11]

2. Results and discussion

$[(N,N)Me_2]_3$TAPB was synthesized through a facile methylation of 1,3,5-tris(4'-aminophenyl)benzene (TAPB) in the presence of K_2CO_3 and excess methyl iodide. The fluorophore was characterized by NMR and mass spectroscopy, and single crystal X-ray measurements.

The absorption spectrum of $[(N,N)Me_2]_3$TAPB in acetonitrile exhibits two prominent absorption bands centred around 205 and 310 nm, which can be attributed to π-π* (S_0-S_2) and n-π* (S_0-S_1) electronic transitions, respectively (See Fig S4). The absorption spectrum is remarkably similar to that of the parent amine TAPB. Addition of PNAC analytes (*i.e.,* TNT, DNT, *m*-DNB, *p*-DNB) to $[(N,N)Me_2]_3$TAPB solution does not change the absorption spectrum. However, addition of the PA has a considerable influence on the absorption spectrum. Fig 1 shows the changes in absorption spectrum upon titrating $[(N,N)Me_2]_3$TAPB against PA in acetonitrile. The absorption band at 205 nm increases in intensity accompanied by marginal blue-shift. On the other hand a new broad band around 375 nm appears, which is due to formation of picrate ions,[10,12] at the expense of 310 nm band. The formation of picrate ions is a consequence of the proton abstraction from PA by $[(N,N)Me_2]_3$TAPB which also diminishes the availability of lone pair of the electrons on -NMe_2 groups and, therefore leads to a decrease in intensity of the 310 nm n-π* band. The residual 310 nm band also appears to have marginal red-shift with the addition of PA. These changes in the absorption spectrum are also accompanied by two isosbestic points at 285 and 327 nm. The isosbestic point at 327 nm can be assigned to the PA and picrate ion equilibrium, while the one at 285 nm can probably assigned to the equilibrium associated with the formation of a complex between the $[(N,N)Me_2]_3$TAPB fluorophore and PA.

The fluorescence spectrum of $[(N,N)Me_2]_3$TAPB exhibits an intense emission at 425 nm upon excitation at 310 nm (λ_{ex}) in acetonitrile solvent (See Fig S4). Unlike TAPB, titration against various PNAC analytes such as TNT, DNT, *m*-DNB, *p*-DNB does not show any significant fluorescence quenching (See Fig S5). On the other hand, fluorescence is

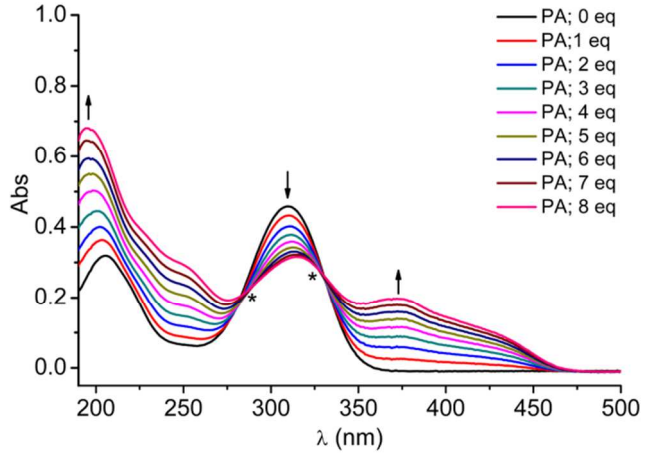

Fig 1. UV-Vis spectra of $[(N,N)Me_2]_3$TAPB (0.4×10^{-5} M) with PA (0 to 8 eq) in acetonitrile (the isosbestic points are shown by asterisks).

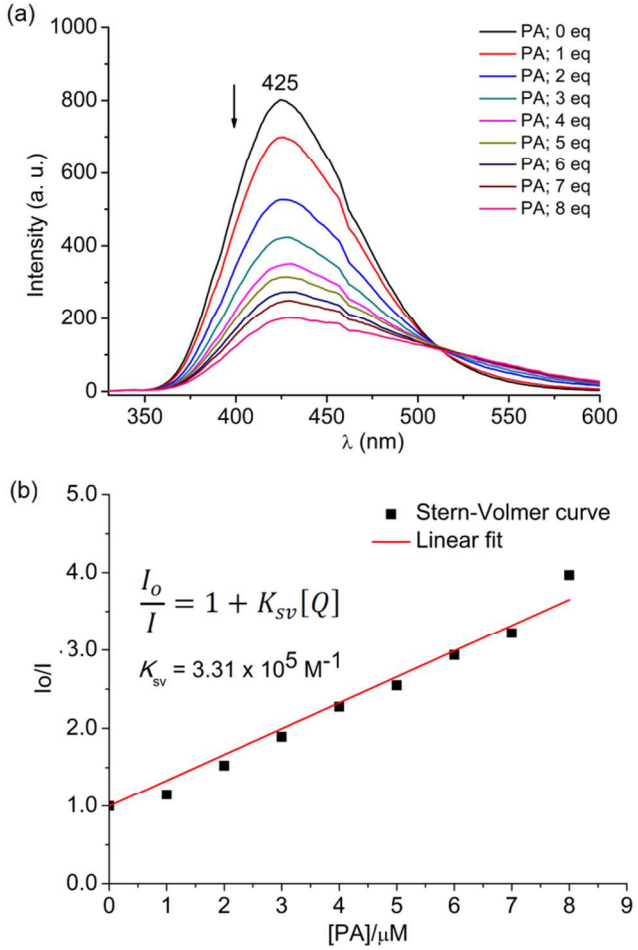

Fig 2. (a) Fluorescence quenching profiles of $[(N,N)Me_2]_3$TAPB in acetonitrile (1.0 μM) with various concentrations of PA and (b) corresponding Stern-Volmer curve.

effectively quenched upon addition of PA. Fig 2(a) shows the changes in the fluorescence spectrum upon titrating $[(N,N)Me_2]_3$TAPB against PA in acetonitrile. Addition of PA accompanied by band broadening, which is indicative of charge transfer characteristics. The fluorescence quenching data were analysed using Stern-Volmer equation and the results are depicted in Fig 2(b). Linearity of the Stern-Volmer plot indicates single mechanism for the quenching process. From the slopes of these curves, quenching efficiencies have been determined in terms of Stern-Volmer constant (K_{sv}). The Stern-Volmer constants for all the PNAC analytes are listed in Table S1. To determine whether the quenching mechanism is static or dynamic, time-resolved fluorescence measurements were carried out. The fluorescence decays of $[(N,N)Me_2]_3$TAPB obtained from the gradual addition of PA (See Fig S6). It exhibits a single exponential decay at λ_{em} = 425 nm with a lifetime of 5.78 ns which remains unchanged upon further additions of PA, which is indicative of static quenching.

The stoichiometry of $[(N,N)Me_2]_3$TAPB-PA complex in solution was determined by Benesi-Hildebrand plot from the fluorescence intensity as a function of PA concentration, which is shown in Fig 3. The Benesi-Hildebrand plot clearly indicates the formation of 1:1 complex between $[(N,N)Me_2]_3$TAPB and PA. The binding affinities determined by fluorescence quenching experiment and the fits to Benesi-Hildebrand

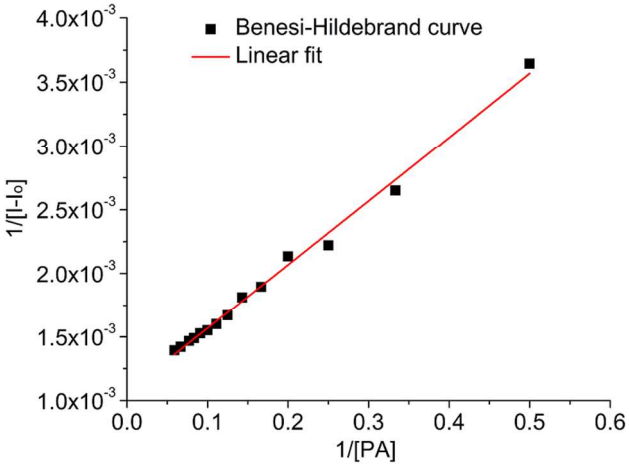

Fig 3. Benesi-Hildebrand plot of $[(N,N)Me_2]_3$TAPB with TNT.

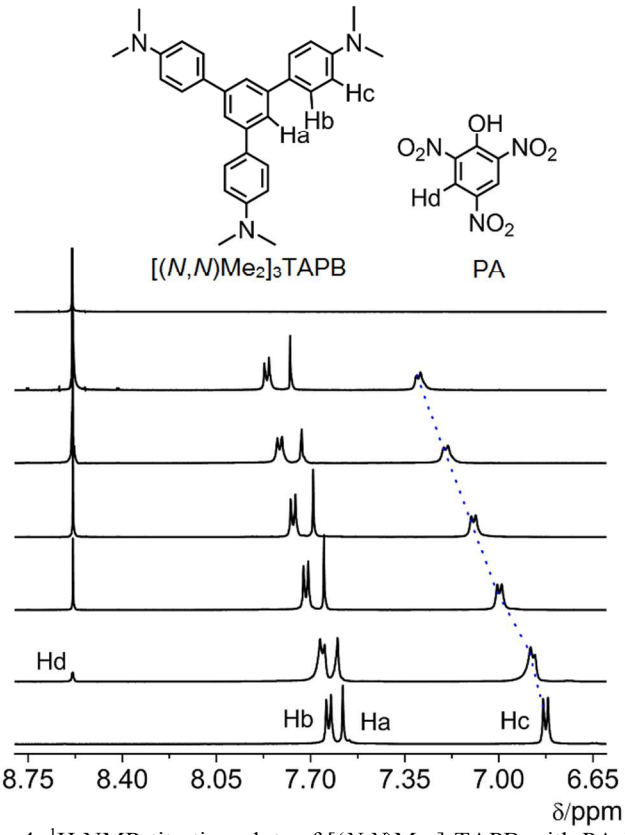

Fig 4. ^{1}H NMR titration plots of $[(N,N)Me_2]_3$TAPB with PA in DMSO-d_6 for Job's plot (peak labelled as "Hc*"* is considered for the calculations).

equation in terms of K_a (association constant) for complexes $[(N,N)Me_2]_3$TAPB with PA, TNT, DNT, *m*-DNB and p-DNB are 2.0×10^8, 9.0×10^5, 6.7×10^5, 6.0×10^5 and 2.5×10^6 M^{-1}, respectively. The association constants are in the order PA >> *p*-DNB > TNT ~ DNT ~ *m*-DNB (See Fig 3 and S8)

^{1}H NMR spectral studies further prove the strong binding of PA with the fluorophore. On titrating $[(N,N)Me_2]_3$TAPB with PA in DMSO-d_6 employing Job's method of continuous variation, gradual downfield shifting of the ^{1}H NMR signals is

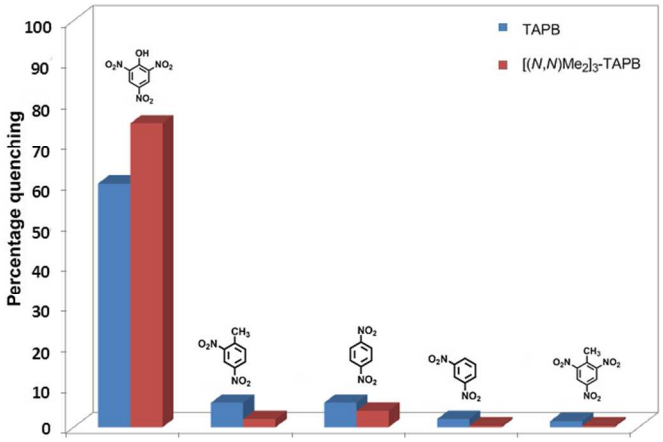

Fig 5. Comparison of the degrees of fluorescence quenching of TAPB and $[(N,N)Me_2]_3$TAPB after addition of PNAC compounds (8 eq each).

observed (Fig 4). Job's plot indicates the complexation of $[(N,N)Me_2]_3$TAPB and PA in a 1:1 stoichiometry (See Fig S7). The observed spectral changes have been rationalized through the formation of electrostatic and hydrogen bond interactions between protonated form of $[(N,N)Me_2]_3$TAPB which possesses strongly desheilding cationic dimethylammonium groups (-$NHMe_2^+$) and picrate anions, formed through proton transfer. The picrate ions form N-H···O with -$NHMe_2^+$ and C-H···O bonds with the activated –CH protons which are *ortho*- and *meta*- to -NMe_2 groups (*i.e.*, H_c and H_b, respectively). The titration with other PNAC compounds (*i.e.,* TNT, DNT, *m*-DNB, and *p*-DNB) do not induce any spectral response, suggesting that $[(N,N)Me_2]_3$TAPB selectively binds only with PA.

Despite having similar structures, $[(N,N)Me_2]_3$TAPB displays significantly lower quenching efficiencies towards TNT, DNT, *m*-DNB and *p*-DNB than those have been observed for the parent fluorophore TAPB.[8] However, in the case of PA the sensitivity of $[(N,N)Me_2]_3$TAPB is higher than parent TAPB. 90% quenching was observed at 32 eq of PA for TAPB and 16 eq of PA for $[(N,N)Me_2]_3$TAPB. The relative quenching efficiencies of TAPB and $[(N,N)Me_2]_3$TAPB after 8 eq of each PNAC analytes are depicted in Fig 5. These results show that the amino groups on the periphery of the TAPB core plays major role in the quenching process by PA.

Photoinduced electron transfer (PET) is the widely accepted mechanism for the fluorescence quenching process.[5,13] In the absence of analyte, the excited electron from HOMO of the fluorophore relaxes back to the ground state with a radiative decay which leads to the origin of the fluorescence. The excited electron can be transferred to LUMO of the PNAC analyte which lies lower in energy than that of the sensor's LUMO. This electron transfer process dominates over the radiative decay to the ground state; substantially quench the fluorescence through non-radiative processes. In order to understand the quenching of the $[(N,N)Me_2]_3$TAPB fluorescence selectively by PA, density functional theory (DFT) calculations were carried out using Gaussian-09 program suite. The geometry optimization and energy calculations were performed using M06-2X hybrid functional of Truhlar and Zhao[14] with 6-311+G(*d*,*p*) basis set for all the atoms.[15] Calculations were carried out both in the gas phase and in acetonitrile solvent (ε = 35.688) using polarized continuum model (PCM). Frontier

Table 1. Calculated energies (eV) of frontier orbitals of $[(N,N)Me_2]_3$TAPB and PNAC analytes.

MO(s)	$[(N,N)Me_2]_3$TAPB	PA	TNT	DNT	*m*-DNB	*p*-DNB
LUMO+1	+ 0.15 (-0.24)	-2.60 (-2.24)	-2.60 (-2.24)	-1.90 (-1.82)	-2.07 (-1.93)	-1.26 (-1.18)
LUMO	+ 0.14 (-0.26)	-3.12 (-2.63)	-2.78 (-2.43)	-2.22 (-2.08)	-2.43 (-2.21)	-2.78 (-2.58)
HOMO	- 6.28 (- 6.57)	-10.03 (-9.51)	-10.47 (-9.98)	-9.80 (-9.44)	-10.18 (-9.74)	-10.11 (-9.65)
HOMO-1	- 6.32 (-6.61)	-10.85 (-10.39)	-10.55 (-10.12)	-10.00 (-9.69)	-10.31 (-9.92)	-10.37 (-9.99)

* Values given in the brackets are obtained from PCM calculations.

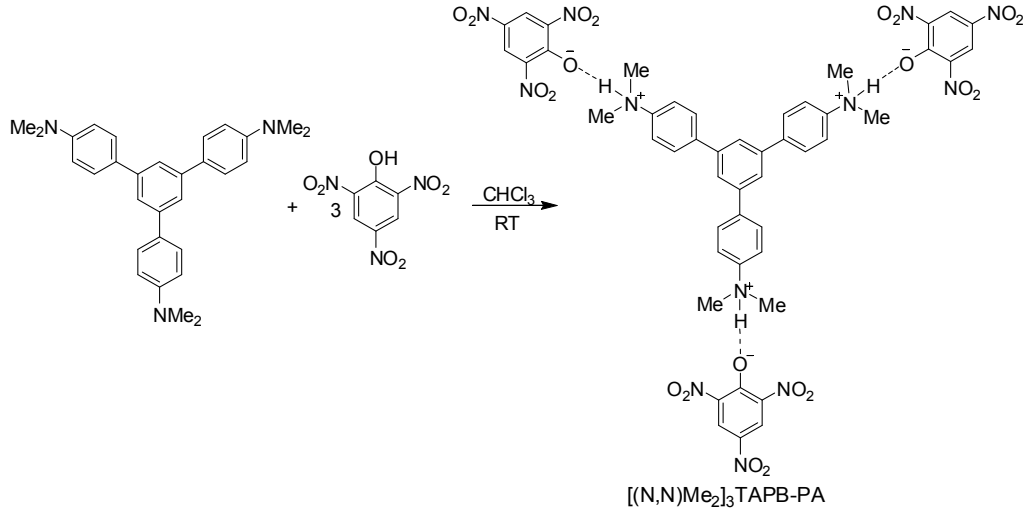

Scheme 1. Preparation of $[(N,N)Me_2]_3$-TAPB-PA complex.

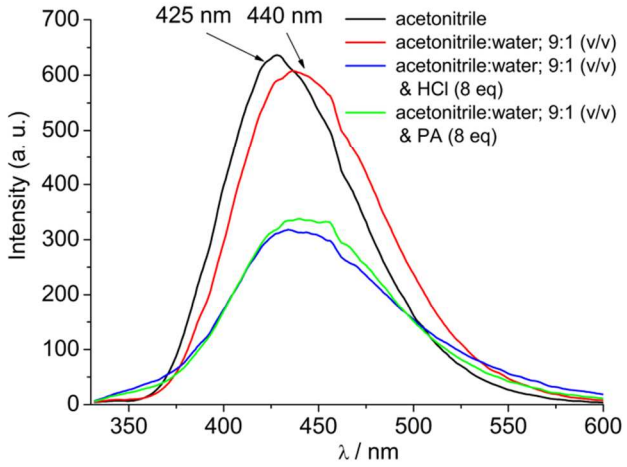

Fig 6. Fluorescence quenching profiles of $[(N,N)Me_2]_3$TAPB (1.0 μM) in acetonitrile, acetonitrile/water mixture in the presence of picric acid and HCl.

orbital energies of $[(N,N)Me_2]_3$TAPB and PNAC analytes have been provided in Table 1. These energies indicate that LUMO of all the analytes have similar energies, which indicate the possibility of fluorescence quenching in all the analytes to be equally probably. However, the fluorescence quenching experiments indicate that PA is almost 25 times more effective quencher in comparison with the other PNAC analytes. The quantum chemical calculations suggest that the the fluorescence quenching of $[(N,N)Me_2]_3$TAPB by PA is not due to PET, unlike the parent TAPB.

In order to undersand the role of proton transfer on the selective fluorescene quenching of $[(N,N)Me_2]_3$TAPB by PA, the fluorescence spectrum of $[(N,N)Me_2]_3$TAPB in aqueous acetonitrile (9:1; v/v) was recorded and the results are shown in Figure 6. The fluoresecne spectrum shows a red-shift of 15 nm in the aqueous acetonitrile. Under these conditions, the addition of 8 eq of PA leads to quenching of the $[(N,N)Me_2]_3$TAPB fluorescence by about 50%, which is lower than the quantum of fluorescence quenching in acetonitrile solvent (about 75%). The difference in the quantum of fluorescence quenching can possibly attributed to the partition coefficient of $[(N,N)Me_2]_3$TAB among water and acetonitrile solvents and the corresponding fluorescence behaviour. It can also be seen from Fig 6 that addition of 8 equivalents of protic acid HCl also leads to similar amount of fluorescence quenching, which clearly establishes the fact that protonation of the fluorophore leads to fluorescence quenching. The selective quenching by PA is attributed to the enhanced basicity of $[(N,N)Me_2]_3$TAPB due to the presence of two methyl groups on the nitrogen atom, which enables abstraction of proton from PA and forms N-H···O ionic hydrogen bond. The present fluorophore has the largest Stern-Volmer constant (K_{SV} = 3.87 × 10^5 M^{-1}). Amongst the several fluorescence sensors for PA reported in the literature the K_{SV} for $[(N,N)Me_2]_3$TAPB is the highest with the exception of hexi-peri-hexabenzocoronene (see Table S4).[16]

To unravel the rationale behind the observed selectivity, solid state structure of the complex of $[(N,N)Me_2]_3$TAPB with PA has been determined using single crystal X-ray diffraction. A 1:3 complex between $[(N,N)Me_2]_3$TAPB and PA was isolated as yellow precipitate from chloroform solvent which was crystallized from acetonitrile to obtain X-ray diffraction quality single crystals (Scheme 1). The complex has been characterized by elemental analysis, NMR spectroscopy and single crystal X-ray diffraction. A single crystal was dissolved in DMSO-d_6 and ^{1}H NMR spectrum was recorded (Fig S11). This ^{1}H NMR spectrum exhibits a singlet at δ 8.58 ppm due to the aromatic protons of the picrate residue. A singlet at δ 7.65

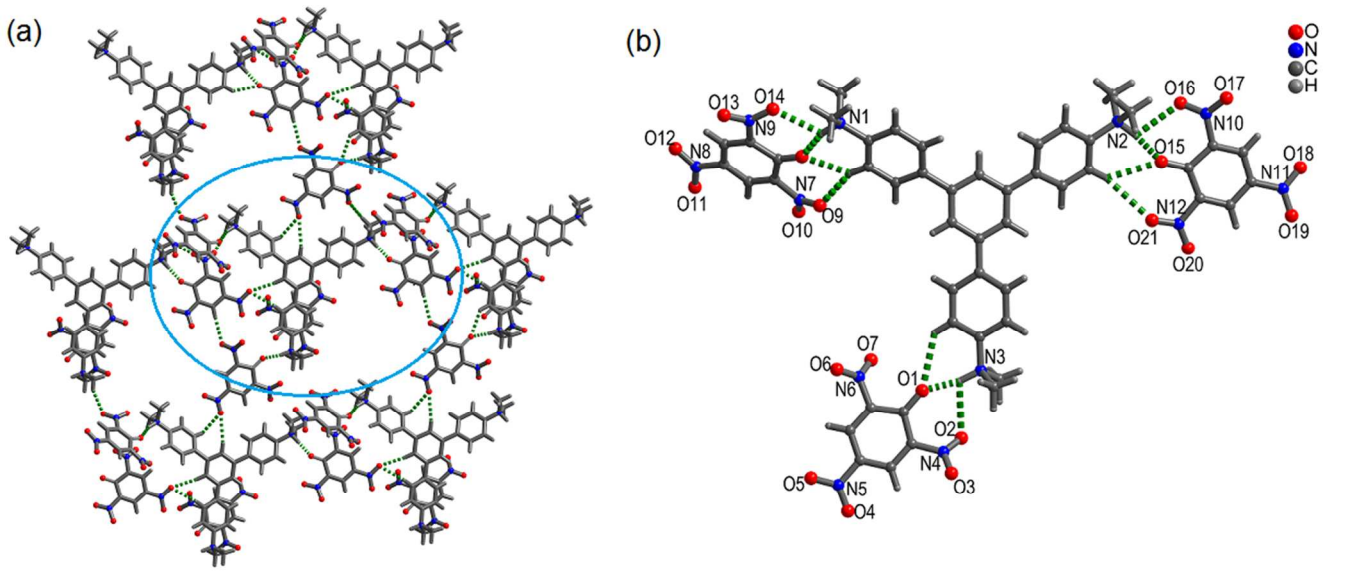

Fig 7. Crystal structure of [(*N*,*N*)Me$_2$]$_3$TAPB-PA complex,(a) Crystal structure of [(*N*,*N*)Me$_2$]$_3$TAPB-PA complex showing hydrogen bonds and π-stacking (H-bonds are shown dashed bonds) and (b) A structural unit.

pm and two doublets at δ 7.8 and 7.15 ppm represent the triphenylbenzene core. The -N(Me$_2$) methyl protons appear as a singlet signal at δ 3.0 ppm. The relative ratio of the intensities of [(*N*,*N*)Me$_2$]$_3$TAPB resonances to PA resonances indicate that the stoichiometry of the complex is 1:3 (see Fig S11).

The [(*N*,*N*)Me$_2$]$_3$TAPB crystallizes as non-planer discrete molecules in monoclinic space group $P2_1/c$ (See Fig S12 and Table S2). The molecules are arranged in loosely packed layers in the crystallographic *bc*-plane and interact with each other by numerous very weak C-H···π interactions (See Table S3 and Fig S13) between N-CH$_3$ groups and aromatic C atoms. The adjacent layers are significantly slipped with improper aromatic stacking. However, they are interconnected by weak aromatic C-H···N hydrogen bonds between centrosymmetry related molecules (See Fig S14) with a shortest distance of *ca* 3.1 Å between the planes passing through their central rings. The crystal structure of [(*N*,*N*)Me$_2$]$_3$TAPB clearly indicates the absence of any supramolecular architecture through strong H-bonding, unlike parent TAPB.

The [(*N*,*N*)Me$_2$]$_3$TAPB-PA complex crystallizes in centrosymmetric triclinic space group *P*-1 with one molecule of [(*N*,*N*)Me$_2$]$_3$TAPB and three molecules of PA in the asymmetric part of the unit cell. The structure indicates that all the three PA molecules have undergone deprotonation by transferring their acidic -OH protons to the -NMe$_2$ groups, resulting in the formation of picrate and triply protonated [(*N*,*N*)Me$_2$]$_3$TAPB species. Each -NHMe$_2^+$ group forms strong N-H···O hydrogen bonds (Table S3) with one picrate residue through phenoxide and one of the *ortho*-NO$_2$ groups as depicted in Fig 7. The activated *ortho*-C-H groups form C-H···O bonds with another *ortho*-NO$_2$ group and phenoxide groups.

The single crystal X-ray diffraction studies reveal the *in situ* formation of picrate ions and protonation of the fluorophore molecules leads to formation of strong ionic hydrogen bond between the fluorophore and PA. This strong ionic hydrogen bond facilitates the PET process (see Fig S15). Similar interactions are not possible with other PNAC compounds tested (no phenolic –OH group) and hence they have much lower fluorescence quenching efficiency in comparison with PA. Attempts to crystalize complexes of [(*N*,*N*)Me$_2$]$_3$TAPB with other PNAC analytes remained unsuccessful.

3. Conclusions

A discrete fluorophore, 1,3,5-tris(4'-(*N*,*N*-dimethylamino)phenyl)benzene was synthesised by a facile methylation reaction TAPB with methyl iodide. This discrete fluorophore shows sensitive and selective fluorescence quenching response to picric acid among other polynitroaromatic analytes. The binding behaviour of picric acid with the fluorophore has been studied by absorption and fluorescence emission and ^{1}H NMR spectroscopic titrations, and single crystal X-ray structure determination. Analysis of X-ray diffraction data reveals that the selectivity of picric acid is originated from the proton transfer from picric acid to the fluorophore. The proton transfer between PA and the fluorophore in non-aqueous solvents is the origin of fluorescence quenching and the resulting selectivity. The results presented in the present investigation hold a great promise for development of new chemo-sensors for selective fluorescence detection of PA.

4. Experimental

4.1. Materials and methods. 2,4-Dinitrotoluene (Sigma-Aldrich), picric acid (Loba Chemie, India), *m*-dinitrobenzene (Thomas Baker, India) and *p*-dinitrobenzene (Specrochem, India), Methods used for purification of solvents were adopted from standard protocols.[17] TAPB was synthesized according to a literature procedure.[18]

4.2. Synthesis of [(*N*,*N*)Me$_2$]$_3$TAPB. Dimethylformamide (dry) solution (2 mL) of TAPB (0.035 g, 0.1 mmol) was added to a suspension of K_2CO_3 (0.25 g, 1.8 mmol) in 10 mL dry dimethylformamide. To this suspension, CH_3I (0.26 g, 3.6 mmol) was added gradually and the resulting mixture was heated at reflux for 3 h. The reaction mixture was cooled to RT

and extracted with diethyl ether (15 mL × 4). The combined organic layers were dried over anhydrous sodium sulphate. The ether solution was kept at RT to obtain needle type crystals suitable for single crystal X-ray diffraction. The crystals were washed with methanol to remove unreacted TAPB. Yield; 0.030 g, 70%. Mp; 255-260 °C. Anal. calcd for $C_{30}H_{33}N_3$: C, 82.72; H, 7.64; N, 9.65. Found: C, 82.36; H, 7.63; N, 9.64. ^{1}H NMR (400 MHz, $CDCl_3$, 295 K): δ 7.63 (s, 3 H, Ar*H*), 7.61 (d, $^3J_{HH}$ = 8.84 Hz, 6 H, Ar*H*), 6.86 (d, $^3J_{HH}$ = 8.72 Hz, 6 H, Ar*H*), 3.0 (s, 18 H, -N(C*H*$_3$)$_2$) ppm. ^{13}C{^{1}H} NMR (400 MHz, $CDCl_3$, 295 K): δ 150.1, 142.2, 130.1, 128.1, 122.8, 113.0, 40.9 ppm. ESI-MS: m/z calcd for $C_{30}H_{34}N_3^+$ $[M + H]^+$ 436.2747, found 436.2750. UV-Vis (CH_3CN); λ_{max} = 203 (ε = 8 × 10^4 M^{-1}cm^{-1}) and 310 (ε = 1.1 × 10^5 M^{-1}cm^{-1}) nm. Emission (CH_3CN); λ_{ex} = 310 nm, λ_{em} = 425 nm.

4.3. Synthesis of [(*N*,*N*)Me$_2$]$_3$TAPBPA. [(*N*,*N*)Me$_2$]$_3$TAPB (0.011 g, 0.025 mmol) was dissolved in chloroform (10 mL). To this, 2 mL chloroform solution of picric acid (0.017 g, 0.075 mmol) was added. A yellow precipitate formed immediately which was filtered out and dissolved in hot acetonitrile and the clear yellow solution was kept at RT for crystallization. Yellow crystals suitable for X-ray diffraction were obtained in two days. Yield; 0.02 g, 71% based on [(*N*,*N*)Me$_2$]$_3$TAPB used. Mp; > 250 °C (dec.). Anal. calcd for $C_{48}H_{72}N_{12}O_{21}$: C, 51.34; H, 3.77; N, 14.97. Found: C, 50.55; H, 3.68; N, 14.10. ^{1}H NMR (400 MHz, DMSO-d_6, 295 K): δ 8.58 (s, 6 H, Ar*H*, picrate), 7.77 (d, $^3J_{HH}$ = 8.72 Hz, 6 H, Ar*H*, [(*N*,*N*)Me$_2$]$_3$TAPB), 7.68 (s, 3 H, Ar*H*, [(*N*,*N*)Me$_2$]$_3$TAPB), 7.10 (d, $^3J_{HH}$ = 8.64 Hz, 6 H, Ar*H*, [(*N*,*N*)Me$_2$]$_3$TAPB), 3.0 (s, 18 H, -N(C*H*$_3$)$_2$,[(*N*,*N*)Me$_2$]$_3$-TAPB) ppm. ^{13}C{^{1}H} NMR (400 MHz, $CDCl_3$, 295 K): δ 160.9, 146.2 (br), 141.9, 141.1, 128.3, 125.3, 124.4, 123.2, 117.1(br), 79.2 ppm. FT-IR (KBr diluted disc); 3434, 1631, 1611, 1316, 1078 cm^{-1}.

4.4. Absorption and emission measurements. UV-Vis absorption spectra were recorded on Varian Cary Bio 100 UV-Vis spectrophotometer. The UV-Vis spectra was recorded using 1.0 × 10^{-5} M solution of [(*N*,*N*)Me$_2$]$_3$TAPB in HPLC grade acetonitrile. The [(*N*,*N*)Me$_2$]$_3$TAPB solution was titrated against increasing concentration of PA (0 to 8 eq). A significant spectral change was observed. All the spectra were overlaid to obtain the complete profile.

The emission spectral studies were performed on Varian 'Cary Eclipse' fluorescence spectrophotometer using quartz cuvette of 1 cm width and scanned for the emission at λ_{ex} = 310 nm, keeping both excitation and emission slit width at 5 nm. 1.0 μM acetonitrile solution of [(*N*,*N*)Me$_2$]$_3$TAPB was titrated against increasing concentration of each PNAC analytes. Emission intensities (I_o) of each analyte were plotted against wavelength to obtain quenching profiles.

Time-resolved fluorescence decay was recorded on a time-correlated single-photon counting system from IBH, UK, with λ_{ex} = 295 nm and the emission polarizer set at a magic angle of 54.7°. The full width at half maximum (FWHM) of the instrument response function (IRF) was 689 ps and the resolution was 7 ps per channel. The data were fitted to single exponential function by the iterative re-convolution method using IBH DAS v6.2 data analysis software to obtain excited state lifetime of [(*N*,*N*)Me$_2$]$_3$TAPB.[19]

4.5. ^{1}H NMR titration. ^{1}H NMR experiments were carried out on a Bruker 500 MHz instrument using DMSO-d_6 (D, 99.9%) as solvent. An amount of 10.50 mg of [(*N*,*N*)Me$_2$]$_3$TAPB and 5.50 mg of PA was dissolved separately in 1.05 mL of DMSO-d_6. The fluorophore solution was divided in seven NMR tubes; 0 μL, 50 μL, 100 μL, 150 μL, 200 μL, 250 μL, 300 μL. To these tubes, the PA solution was added in such a way that sum of both the concentrations remains constant in all the tubes. Gradual downfield shifting of all the ^{1}H NMR peaks of [(*N*,*N*)Me$_2$]$_3$TAPB was observed. Job's plot was obtained by plotting Δδ.Δx v/s Δx where Δδ is the difference in chemical shift between free fluorophore and the observed values for complex, and Δx is the corresponding mole fraction of the fluorphore. The stoichiometry of the complex was obtained from the value of the molar fraction Δx which corresponds to a maximum of the curve: a 1:1 complexation is obtained for Δx_{max} = 0.5.

4.6. X-ray crystallography. The X-ray diffraction data were collected on a Rigaku Saturn 724 HG CCD diffractometer with a Mo-Kα radiation source (λ = 0.71075 Å) at 150 K under continuous flow of cooled nitrogen gas. The structures were solved by direct methods using *SIR*- 92[20] and refined by full-matrix least-squares fitting on F^2 using *SHELX*-97.[21] All non-hydrogen atoms were refined anisotropically. The hydrogen atoms were refined isotropically as rigid atoms in their idealized locations. The N-H protons of [(*N*,*N*)Me$_2$]$_3$TAPB-PA were located from difference Fourier maps, and refined independently. The detailed information about the refinement is given in Table S2.

4.7. DFT calculations. All the theoretical calculations were performed using Gaussian 09 program packages with its graphical interface GAUSSVIEW-05. The gas phase geometries were optimized with unrestricted density functional theory using M06-2X/6-311+G(*d,p*) level of calculation.

5. Acknowledgements

We thank the SERB/DST-New Delhi and the DAE-Mumbai, India for financial support. P V and S S are thankful to CSIR-New Delhi for their fellowships. We gratefully thank Prof. Anindya Datta for valuable discussion on the photophysical studies.

Notes

Department of Chemistry,
Indian Institute of Technology Bombay, Mumbai, India-400 076
G. Naresh Patwari
Email; naresh@chem.iitb.ac.in
Ramaswamy Murugavel
Email; rmv@chem.iitb.ac.in

Supporting information

Electronic Supplementary Information (ESI) available: NMR spectra, ESI-MS spectrum, crystal packing diagrams, UV-Vis spectrum, additional fluorescence spectra, crystallographic data in CIF format; Crystallographic data have also been deposited with Cambridge Crystallographic Data Centre; CCDC numbers 1010527-1010528. See DOI: 10.1039/b000000x/

6. References

(1) (a) R. Murugavel and R. Pothiraja, *New J. Chem.,* 2003, **27**, 968-974; (b) R. Murugavel, S. Kuppuswamy, N. Gogoi andA. Steiner,*Inorg. Chem.*, 2010, **49**, 2153-2162; (c) G. Prabusankar, R. Murugavel andR. J. Butcher, *Organometallics*, 2004, **23**, 2305-2314; (d) R. Murugavel and M. P. Singh, *New J. Chem*., 2010, **34**,

1846-1854; (e) R. Murugavel andS. Shanmugan, *Chem. Commun*., 2007, 1257-1259; (f) S. Banerjee, S. Shanmugan and R. Murugavel,*Struct. Chem*., 2007, **18**, 165-169.
(2) B. Szczęsna and Z. Urbańczyk-Lipkowska, *New J. Chem*., 2002, **26**, 243-249.
(3) (a) F. H. Allen, V. J. Hoy, J. A. K. Howard, V. R. Thalladi, G. R. Desiraju, C. C. Wilson and G. J. McIntyre, *J. Am. Chem. Soc*., 1997, **119**, 3477-3480; (b) P. K. Thallapally, A. K. Katz, H. L. Carrell andG. R. Desiraju, *Chem. Commun*., 2002, 344-345; (c) P. K. Thallapally, A. K. Katz, H. L. Carrelland G. R. Desiraju, *CrystEngComm,* 2003, **5**, 87-92.
(4) J. Wu, W. Liu, J. Ge, H. Zhangand P. Wang, *Chem. Soc. Rev*., 2011, **40**, 3483-3495.
(5) N. Niamnont, N. Kimpitak, K. Wongravee, P. Rashatasakhon, K. K. Baldridge, J. S. Siegel and M. Sukwattanasinitt, *Chem. Commun*., 2013, **49**, 780-782.
(6) T. W. Panunto, Z. Urbanczyk-Lipkowska, R. Johnson andM. C. Etter, *J. Am. Chem. Soc.*,1987, **109**, 7786-7797.
(7) (a) S. Shanmugaraju, H. Jadhav, R. Karthik and P. S. Mukherjee, *RSC Advances*, 2013, **3**, 4940-4950; (b) B. Gole, S. Shanmugaraju, A. K. Bar, P. S. Mukherjee, *Chem. Commun*., 2011, **47**, 10046-10048; (c) J.-D. Xiao, L.-G. Qiu,F. Ke, Y.-P. Yuan, G.-S. Xu, Y.-M. Wang, X. Jiang, *J. Mater. Chem. A*, 2013, **1**, 8745-8752.
(8) P. Vishnoi, M. G. Walawalkar, S. Sen, A. Datta, G. N. Patwari and R. Murugavel, *Phys. Chem. Chem. Phys.* 2014, **16**, 10651-10658.
(9) (a) V. Bhalla, A. Gupta, M. Kumar, D. S. S. Rao and S. K. Prasad, *ACS Appl. Mater. Interfaces*, 2013, **5**, 672-679; (b) J. F. Wyman, M. P. Serve, D. W. Hobson, L. H. Lee and D. E. Uddin, *J. Toxicol. Environ. Health Part A* 1992, **37**, 313-327; (c) H.-T. Feng, Y.-S. Zheng, *Chem. Eur. J.,* 2014, **20**, 195-201.
(10) (a) J. Shen, J. Zhang, Y. Zuo, L. Wang, X. Sun, J. Li, W. Han and R. J. He, *Hazard. Mater*., 2009, **163**, 1199-1205; (b) M. Kumar, S. I. Rejaand V. Bhalla, *Org. Lett.*, 2012, **14**, 6084-6087.
(11) (a) M. Laurenti, E. López-Cabarcos, F. García-Blanco, B. Frick andJ. Rubio-Retama, *Langmuir*, 2009, **25**, 9579-9584; (b) D. R. Shankaran, K. V. Gobi, K. Matsumoto, T. Imato, K. Toko and N. Miura, *Sens. Actuators B*, 2004, **100**, 450-454; (c) S.-Z. Tan, Y.-J. Hu, J.-W. Chen, G.-L. Shen and R.-Q. Yu, *Sens. Actuators B*, 2007, **124**, 68-73.
(12) B. M. Rambo, S. K. Kim, J. S. Kim, C. W. Bielawski, and J. L. Sessler, *Chemical Science*, 2010, **1**, 716-722.
(13) (a) D. A. Olley, E. J. Wren, G. Vamvounis, M. J. Fernee, X. Wang, P. L. Burn, P. Meredith and P. E. Shaw, *Chem. Mater*., 2011, **23**, 789–794; (b) X. Liu, Y. Xu and D. Jiang, *J. Am. Chem. Soc.*, 2012, **134**, 8738–8741.
(14) G. He, H. Peng, T. Liu, M. Yang, Y. Zhang and Y. Fang, *J. Mater. Chem*., 2009, **19**, 7347-7353.
(15) D. Li, J. Liu, R. T. K. Kwok, Z. Liang, B. Z. Tang and J. Yu, *Chem. Commun.*, 2012, **48**, 7167-7169.
(16) V. Vij, V. Bhalla, and M. Kumar, *ACS Appl. Mater. Interfaces*, 2013, **5**, 5373-5380.
(17) Purification of Laboratory Chemicals, D. D. Perrin, Armarego W.L.F.; Pergamon Press; 3rd Ed. 1988.
(18) C. Bao, R. Lu, M. Jin, P. Xue, C. Tan, T. Xu, G. Liu and Y. Zhao, *Chem. Eur. J*., 2006, **12**, 3287-3294.
(19) T. K. Mukherjee and A. Datta, *J. Phys. Chem. B*, 2006, **110**, 2611-2617.
(20) A. Altomare, G. Cascarano, C. Giacovazzo and A. Guagliardi, *J. Appl. Crystallogr.* 1993, **26**, 343-450.
(21) G. M. Sheldrick, *Acta Crystallogr*. 2008, **A64**, 112-122.

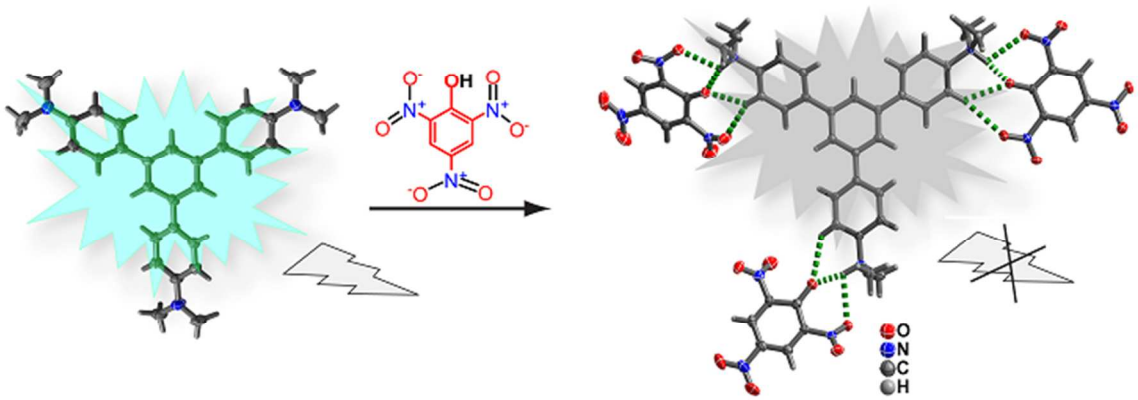

A new triaminophenylbenzene based fluorescent chemo-sensor has been synthesized and successfully employed for the selective fluorescence detection of picric acid.